

Christian Reyner<sup>1</sup>, Conan Lee<sup>1</sup>, Dajung Kim<sup>1,2</sup> & Rhea P. Liem<sup>1</sup>

<sup>1</sup>The Hong Kong University of Science and Technology, Kowloon, Hong Kong SAR <sup>2</sup>Ecole Nationale de l'Aviation Civile, Toulouse, France

### **Abstract**

Propeller selection plays an important role in determining the overall performance of small Unmanned Aerial Vehicles (sUAVs). Due to the variability of operational conditions, selecting the optimal propeller for sUAVs from a pool of available propeller choices in the market—could be a challenging task. In this paper, we propose a methodology for addressing these issues via a systematic method to maximize the overall efficiency of sUAVs during a mission, which includes vertical take-off and landing (VTOL). The proposed methodology involves overall performance efficiency evaluation for VTOL sUAVs operating in natural disturbances, where flight data analysis is performed using a combined unsupervised machine learning (ML) algorithm and surrogate models to perform inverse calculations of the required thrust. The ML technique clusters flight conditions to reduce the amount of information from flight data while maintaining the important features of the mission. The surrogate model, which improves computational efficiency, is used to predict the overall performance efficiency of sUAVs under various flight conditions during the entire mission. The proposed methodology can provide a more rigorous quantitative basis for the optimal propeller selection in an efficient manner. In the future, the methodology can also be extended to enable the numerical optimization of the overall performance for sUAVs design based on the real operational environment.

Keywords: VTOL, sUAV, propeller selection, mission-based optimization, data driven

### **Nomenclature**

Dpropeller diameter (in)

J advance ratio P power (W)

Ρi

= propeller pitch (in) thrust (kgf)

TPR = thrust to power ratio (g/W)

= airspeed (m/s)V

efficiency = η

proportion of segment

## 1 Introduction

Small unmanned aerial vehicles (sUAVs), specifically the convertible vertical take-off and landing (VTOL) configurations, have gained popularity in recent years due to their versatility for a wide range of applications in various fields, such as surveillance [1], agriculture [2, 3], and delivery services [4]. To support these usages, there are a wide range of sUAV components in the market. However, identifying the optimal combination of those components to fulfil a specific mission remains a challenge, due to the complex interactions among them. In particular, selecting the optimal propeller of VTOL sUAVs is difficult due to the diversity of available propellers and the complexity of quantifying overall efficiency in various operational configurations. Hence, developing a systematic, quantitative optimization method is crucial in light of the importance of propeller selection for designing energy-efficient sUAVs.

The traditional method for propeller selection, commonly implemented for piston-powered aircraft, typically involves extensive testing and/or simulation for both the aircraft and the propellers to obtain the optimal design [5]. Researchers have attempted to develop similar methods for the selection and design of UAV propellers. According to the review paper by Patel *et al.* [6], common methods employed are computational fluid dynamics (CFD) and experimental testing. Of these currently available methods, numerical simulation by CFD is the most effective and efficient in analyzing propeller geometry forces and efficiency. However, applying it to select sUAVs' propellers is time-consuming and costly.

In the context of VTOL sUAVs' propeller selection, flight condition distribution is one of the essential factors to take into account. sUAVs often operate in many different flight mission profiles and conditions. Furthermore, VTOL sUAVs operate vertically at take-off and landing, before converting to the cruise mode. Flight conditions in these diverse states represented by speed and required thrust can vary significantly based on the type of mission and natural disturbances, such as wind or aircraft degradation. Hence, the optimal point changes throughout a mission as flight conditions vary, raising the need for optimization. Yet, we observe that this important consideration is often missing in most methods presented in the literature.

In this study, we propose an efficient computational methodology to select an optimal propeller for VTOL sUAVs performing certain missions. This mission-based optimization approach involves flight data analysis, an overall efficiency formulation for VTOL configurations, and optimization problem formulations. Flight data containing information on natural disturbances and missions are first categorized into mission segments using a combined unsupervised ML algorithm. The required thrust is then estimated through an inverse parameter calculation of the clustered data. Subsequently, the overall efficiency is computed using the surrogate model of the propeller datasets. Ultimately, the optimal diameter and pitch of the propeller are selected from the efficiency map built using a surrogate modeling technique upon the manufacturers' data. This proposed methodology facilitates the numerical optimization of the overall efficiency of VTOL sUAVs under real operational conditions. Additionally, the methodology reduces the time and cost associated with selecting an optimal propeller compared to the "trial and error" approach, which is commonly applied in current practice.

This paper is structured as follows. The details of the specific challenges in the current VTOL sUAV configuration will be further elaborated in Section 2. The proposed methodology that provides a quantitative basis for a rigorous propeller selection, which ensures optimal performance throughout the vehicle's operations, will be explained in Section 3. A test case and results from the proposed approach, which shows the potential improvements in mission efficiency, are presented in Section 4 and followed by the final remarks in Section 5.

# 2 Overview of VTOL Configurations and Their Performances

In this section, we provide an overview of current VTOL configurations in sUAV and present the formulation to evaluate the efficiency of the propulsion system in this configuration. Particularly, the challenges in prospective convertible VTOL configuration, electric propulsion system, and sUAV propeller within each subsection will be discussed.

# 2.1 VTOL sUAV Configuration

Aerial vehicles can generally be categorized into two types based on their main lifting mechanisms, namely fixed-wing (FW) and rotary-wing (RW) configurations. They offer different capabilities in terms of endurance and flexibility, which mainly stem from their distinct take-off and landing performances. Their distinct configurations bring about their unique set of advantages and disadvantages. As an example, fixed-wing aircraft are generally faster and have longer endurance due to their efficient aerodynamics, but they require a runway for take-off and landing. On the other hand, rotary-wing aircraft can take off and land vertically, making them more flexible in terms of operating in confined spaces, but they have shorter endurance and are less efficient in forward flight. To overcome their own limitations, researchers came up with the idea of merging these two configurations, forming the hybrid aircraft known as VTOL FW Aircraft; a well-known example is the V-22 Osprey, which was first flown in 1989.

The advancement of unmanned technology allows researchers to further explore hybrid configurations more rapidly, resulting in numerous designs and VTOL configurations. Some common sUAV configurations that currently dominate the market are shown in Fig. 1 [7, 8, 9, 10]. An extensive study comparing designs and flight control techniques of VTOL UAVs can be found in a review paper by Ducard and Allenspach [11]. In their study, they examined several configurations, from the independent VTOL configuration (separate propulsion system) to the convertible configuration (tilt wing, tilt-rotor, and tail sitter).

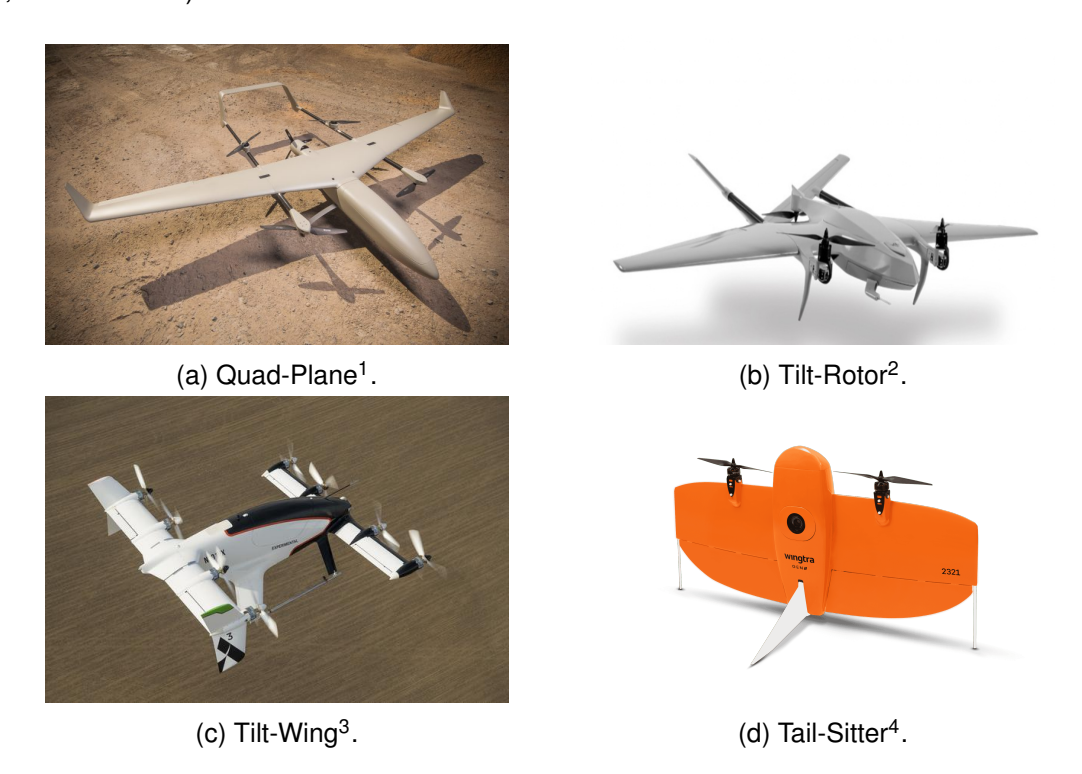


Figure 1 – Independent (a) and convertible (b)(c)(d) propulsion system configurations in VTOL aircraft.

From the design perspective, the three configurations (namely independent, convertible, and their combinations) have their own advantages and disadvantages, with none being truly superior to the others. The drive to improve performance has led the UAV industry to focus on the development of convertible types, particularly in the sUAV category [12], due to its potential for weight reductions. In this paper, we will focus on convertible-type VTOL sUAVs, particularly the tilt-rotor configuration.

Figure 2 shows the typical structure of the VTOL sUAVs electric propulsion system. The key components of this system are the propeller, the motor, the motor controller, and the battery, which all play critical roles in the aircraft's performance efficiency. While some sUAVs may also include additional avionic devices that might draw additional energy along the flight, this subsection will focus specifically on the propulsion system components illustrated in Fig. 2.

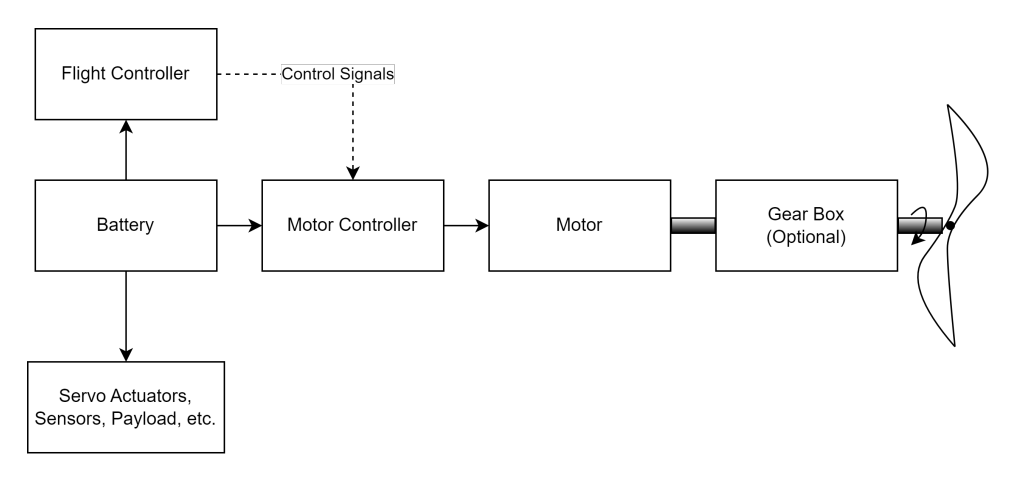


Figure 2 – Typical electric UAV propulsion system.

# 2.2 Fixed-Pitch Propeller Efficiency in Convertible Configuration

The two distinguished configurations mentioned in Section 2.1, namely fixed-wing and rotary-wing aircraft, encounter two different conditions, i.e., dynamic thrust and static thrust conditions. In multirotor, when performing hover, there is no apparent wind relative to its propeller; thus, the propeller in hover condition generates the static thrust. On the other hand, in moving fixed-wing aircraft, the propeller generates dynamic thrust because of its relative wind to its propeller. Although both of these phenomena look the same from the propeller's dynamic points of view, the required pitch to efficiently generate static and dynamic thrust are totally different. The propeller in static thrust conditions performs best with low or fine pitch, while the cruising phase requires a much higher pitch to acquire high efficiency [13]. One of the major drawbacks of using the convertible VTOL configuration is the requirement to deal with hover and cruise with the same propulsion system, as the configuration required for each mode conflicts with the other.

The mathematical definition of propeller aerodynamic coefficients and efficiency are presented in Eq. (1), following the work presented in [14].

$$C_T = \frac{T}{\rho n^2 D^4}, \qquad J = \frac{V}{nD},$$
 
$$C_P = \frac{P}{\rho n^3 D^5}, \qquad \eta = J \frac{C_T}{C_P} = \frac{TV}{P_{\text{mech}}},$$
 (1)

<sup>1</sup> https://www.altiuas.com (last accessed on 22 November 2023).

<sup>&</sup>lt;sup>2</sup>https://www.beta-uas.id/raybe (last accessed on 22 November 2023).

 $<sup>^3</sup>$ https://www.airbus.com/en/innovation/low-carbon-aviation/urban-air-mobility/

cityairbus-nextgen/vahana (last accessed on 22 November 2023).

<sup>&</sup>lt;sup>4</sup>https://wingtra.com/drone-wingtraone (last accessed on 22 November 2023).

where the advance ratio J is defined as the ratio of the apparent airspeed V to the tip speed nD of the propeller. Here, n represents the number of revolutions per second, and D denotes the propeller diameter. The thrust coefficient  $C_T$  and power coefficient  $C_P$  are dimensionless variables derived from dimensional analysis and play a crucial role in the analysis of propeller performance.  $\rho$  is air density, T is thrust, and P is pressure. The propeller efficiency  $\eta$  is defined as the ratio of the aerodynamic power  $P_{\text{aero}} = TV$  to the mechanical power  $P_{\text{mech}}$ .

It is noted that propeller efficiency  $\eta$  does not directly translate into propeller performance under static or hovering conditions. As the apparent airspeed is equal to zero under static conditions, resulting in J=0, the efficiency also consequently drops to zero, resulting in an unknown and immeasurable condition, according to the previous definition in Eq. (1). In industry practice, a metric described by the ratio of generated thrust and mechanical power,

$$\mathsf{TPR} = \frac{T}{P_{\mathsf{mech}}},\tag{2}$$

is preferred to describe the efficiency in static conditions.

The thrust-to-power ratio, TPR, defined in Eq. (2), is a practical approach to describe static efficiency. As an example, comparing two propellers or propulsion setups with the TPR of 10 g/W and 8 g/W for an aircraft with a hover thrust requirement of 1 kg, yields to 100 W and 125 W of the power requirement, respectively. It gives the direct transformation between the required thrust and required power for hovering, intuitively showing the static efficiency.

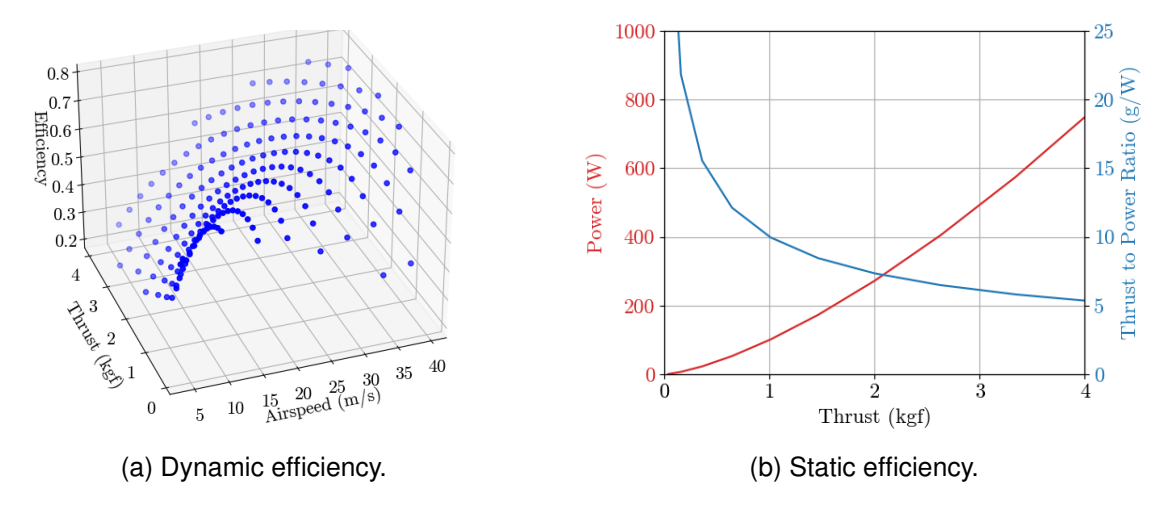


Figure 3 – Efficiency curves of the propeller: dynamic and static efficiency as a function of aircraft operating conditions.

Figure 3 shows the example of the dynamic and static efficiencies of APC 10x6 propeller, presented using the definition from Eq. (1) and Eq. (2), repectively. Both efficiencies are presented with variations of the aircraft operating conditions: the required thrust and airspeed for the dynamic efficiency in Fig. 3a and the required thrust for the static efficiency in Fig. 3b.

# 3 Proposed Mission-Based Analysis Methodology

The flight conditions of VTOL sUAVs vary from mission to mission. Figure 4 shows some of the mission examples, ranging from a simple waypoint following mission, such as Figs. 4a and 4b, to a very complex aerial mapping mission, such as Figs. 4c and 4d. Specifying a mission and taking into account flight condition changes throughout the mission play an important role in achieving the optimal selection of the propeller. As the optimal conditions for each mission can be different from each other, performing a mission-based analysis is important to address the diverse conditions of each mission configuration.

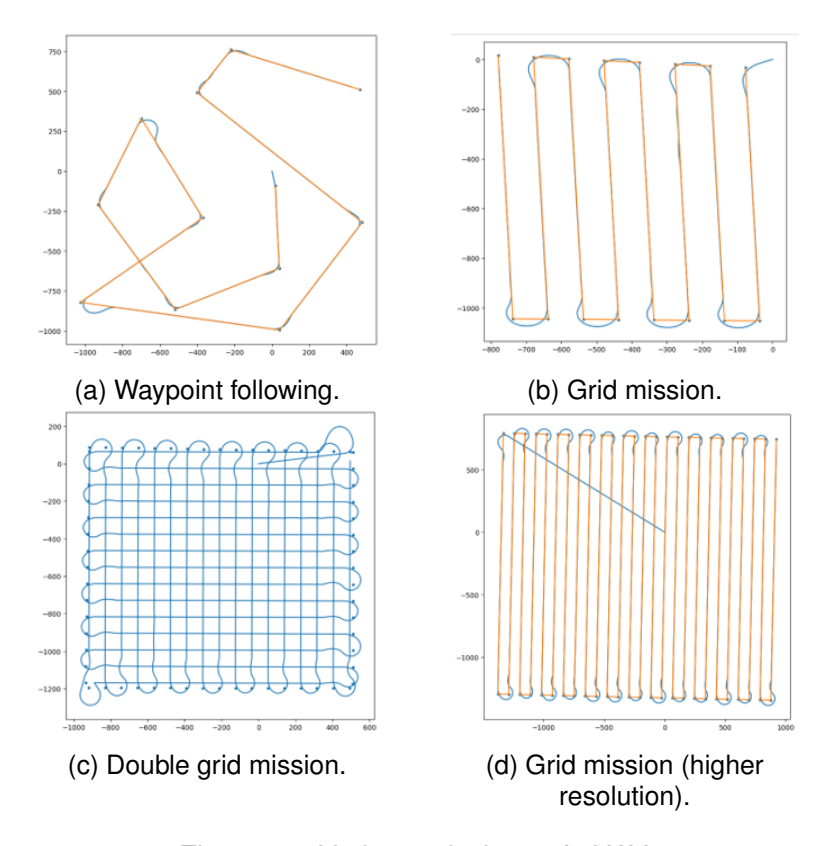


Figure 4 – Various missions of sUAV.

Despite the projected benefits, mission-based analysis in sUAV poses several challenges due to the large amount of data to be processed, uncertainty in the measurements, and the limited availability of sensors. As an example, the conventional sUAV flight controller performs the measurement at 10Hz, which means that an hour of flight results in 36,000 data. Aircraft also do not fly at an ideal steady condition, even in one flight segment. There are natural disturbances that might cause fluctuations in the flying speed and required thrust. Furthermore, commercial sUAVs are equipped with standard minimum instruments only to monitor their remaining "fuel" and flight status; however, these do not directly provide the required variables for calculating the efficiency of the propeller. Adding dedicated sensors to monitor the efficiency might be possible but not practical.

In this section, we introduce the framework for overcoming the challenges mentioned above. The overview of the whole process is presented in Fig. 5. There are three main components to obtain the optimal propeller selection for VTOL sUAVs. The first one is the problem reduction technique that incorporates multiple clustering algorithms, taking into account the joint probability distribution for more accurate representation, as described in Section 3.1. The second component is the surrogate modeling technique, as seen later in Section 3.2, to obtain the low-cost yet accurate model of the propeller performance model for raw flight data processing and the later optimal propeller evaluation. The last one is to evaluate and obtain the optimal propeller selection, which is described in Section 3.3.

## 3.1 Flight Data Clustering

Clustering flight data helps overcome the problem of solving large data sets in mission-based analysis while retaining the information for flight phases/regimes. Flight data from UAV can be vast, with more than 36,000 data points recorded during an hour flight with more than 10Hz sampling rate. Clustering algorithms can group these data points into several clusters, allowing the identification of patterns and trends within the flight data. Flight data clusters provide insights into distinct operational phases. Clustering enables the optimization of performance and efficiency, and assists in the development of customized strategies and algorithms for specific flight regimes.

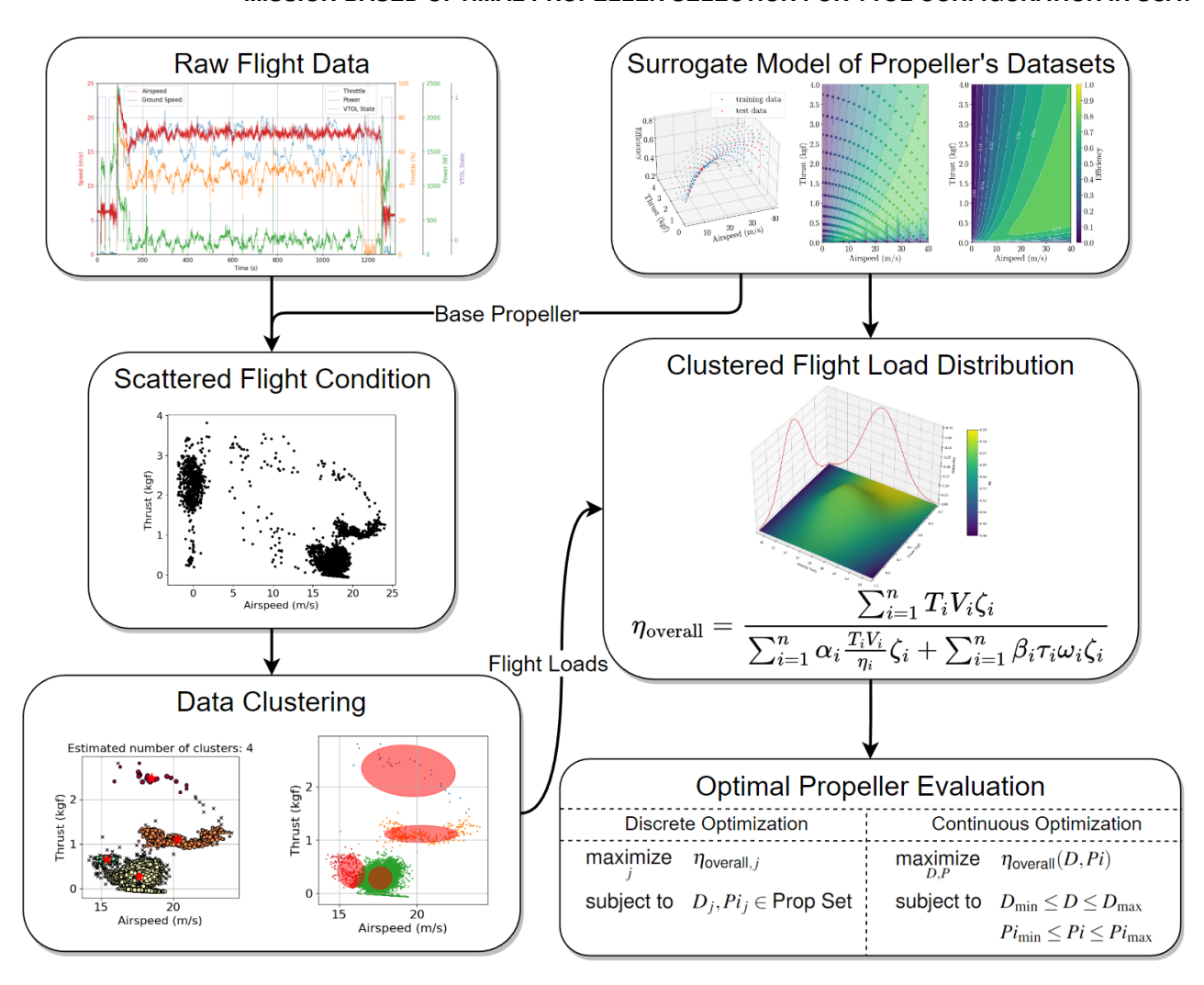


Figure 5 – Mission-based optimal propeller selection process.

Identified patterns and trends can further be used to optimize the propeller selection process, leading to better UAV performance compared to typical single/multi-point optimization analysis. Overall, clustering flight data is an essential technique for improving the performance and efficiency of UAVs.

The study on the use of the clustering method in flight data analysis was demonstrated by Liu *et al.* [15]. They found that the Gaussian Mixture Model (GMM) algorithm performed the best in recognizing the flight phase. They also showed that the use of this algorithm in flight data clustering could provide valuable insights into flight load in different flight conditions.

The GMM is a clustering algorithm that assumes the data points are generated from a mixture of Gaussian distributions with unknown parameters. It can be seen as an extension of k-means clustering, as it incorporates information about the covariance structure of the data and the centers of the latent Gaussians. A Gaussian distribution is often used to represent the continuous probability distribution in probability theory. The general form of its probability density function is as follows.

$$p(x) = \frac{1}{\sigma\sqrt{2\pi}}e^{-\frac{(x-\mu)^2}{2\sigma^2}}.$$
 (3)

The parameter  $\mu$  is the mean or expectation of the distribution, while the parameter  $\sigma$  is the standard deviation of the distribution. This distribution is often used to represent an unknown variable, such as natural disturbances in an expected steady condition.

The utilization of the GMM, however, requires a known number of clusters as its input, which can greatly vary depending on the mission type, and the mission configuration can be totally different from

one to another in sUAV operations. Hierarchical Density-based Spatial Clustering of Applications with Noise (HDBSCAN) and Ordering Points To Identify the Clustering Structure (OPTICS) algorithms can deal with the unknown number of clusters. Both have their own strengths; however, the HDBSCAN algorithm is better suited for our practical application as it has better algorithm than OPTICS in terms of time complexity.

In this study, the combination of HDBSCAN and GMM from scikit-learn package from the scikit-learn library<sup>1</sup> is used to solve the underlying problem in the GMM algorithm, which is the unknown number of clusters. The combination of these two methods can also be useful in providing a simplified but accurate representation of the flight load of the aircraft throughout its flight. Furthermore, the utilization of GMM addresses the disturbances along the flight, assuming that the distribution of the natural disturbances to the aircraft will follow a normal distribution.

The efficiency of the propeller is defined as the function of the required thrust and the airspeed, which represent the operational conditions. Considering the disturbance in both thrust and airspeed data as the probability function  $f_{T_iV_i}(T,V)$  at cluster i, the joint probability density function of the propeller's efficiency  $F(T_i,V_i)$  in continuous form is as follows:

$$F(T_i, V_i) = \int \int_{\mathbb{R}} f_{T_i V_i}(T, V) d_T d_V,$$
where 
$$\int_{-\infty}^{\infty} \int_{-\infty}^{\infty} f_{T_i V_i}(T, V) d_T d_V = 1.$$
(4)

Transforming the continuous probability function into discrete form, the joint probability function is expressed by the following equations:

$$F(T_i, V_i) = \sum_{\mathbb{R}} \int_{T_i V_i} f_{T_i V_i}(T, V),$$
 where 
$$\sum_{T} \sum_{V} f_{T_i V_i}(T, V) = 1.$$
 (5)

Following the power consumption model for the electric aircraft, the efficiency of each cluster is expressed as follows:

$$\begin{split} P_{\mathsf{aero}_i} &= \sum_{T} \sum_{V} P_{\mathsf{aero}}(T, V) f_{T_i V_i}(T, V) \\ &= \sum_{T} \sum_{V} TV f_{T_i V_i}(T, V), \end{split} \tag{6}$$

$$\begin{split} P_{\mathsf{mech}_i} &= \sum_{T} \sum_{V} \frac{P_{\mathsf{aero}}(T, V)}{\eta(T, V)} f_{T_i V_i}(T, V) \\ &= \sum_{T} \sum_{V} \frac{TV}{\eta(T, V)} f_{T_i V_i}(T, V), \end{split} \tag{7}$$

$$\eta_i = \frac{\sum_T \sum_V TV f_{T_i V_i}(T, V)}{\sum_T \sum_V \frac{TV}{\eta(T, V)} f_{T_i V_i}(T, V)}.$$
(8)

Furthermore, the overall efficiency for the whole mission is solved by combining the power consumption from each cluster as follows:

$$P_{\text{aero}} = \sum_{i=1}^{n} P_{\text{aero}i} \zeta_i = \sum_{i=1}^{n} T_i V_i \zeta_i, \tag{9}$$

$$P_{\text{mech}} = \sum_{i=1}^{n} \frac{P_{\text{aero}i}}{\eta_i} \zeta_i = \sum_{i=1}^{n} \frac{T_i V_i}{\eta_i} \zeta_i, \tag{10}$$

$$\eta_{\text{overall}} = \frac{P_{\text{aero}}}{P_{\text{mech}}} = \frac{\sum_{i=1}^{n} T_i V_i \zeta_i}{\sum_{i=1}^{n} \frac{T_i V_i}{\eta_i} \zeta_i}.$$
(11)

<sup>&</sup>lt;sup>1</sup>https://scikit-learn.org/stable/modules/clustering.html (last accessed on 15 April 2024).

The above expression for  $\eta_{\text{overall}}$  (where  $\zeta_i$  represents the proportion of time spent in a flight segment) does not account for the efficiency in the static condition, when the  $\eta_i$  and  $V_i$  are equal to zero. To address this, the mechanical power at static condition,  $P_{\text{mech, static}}$ , can be expressed by using torque,  $\tau$ , and angular velocity,  $\omega$ :

$$P_{\text{mech, static}} = \sum_{i=1}^{n} \tau_i \omega_i \zeta_i$$
 (12)

To distinguish between the dynamic and static conditions, we introduce indicator functions  $\alpha_i$  and  $\beta_i$ :

$$\alpha_i = \begin{cases} 1 & \text{if the } i\text{-th segment is a dynamic segment} \\ 0 & \text{otherwise}, \end{cases} \tag{13}$$

$$\beta_i = \begin{cases} 1 & \text{if the } i\text{-th segment is a static segment} \\ 0 & \text{otherwise.} \end{cases}$$
 (14)

The total mechanical power is then:

$$P_{\text{mech}} = P_{\text{mech, dynamic}} + P_{\text{mech, static}} = \sum_{i=1}^{n} \alpha_i \frac{T_i V_i}{\eta_i} \zeta_i + \sum_{i=1}^{n} \beta_i \tau_i \omega_i \zeta_i.$$
 (15)

By incorporating this value into Eq. (11),  $\eta_{\text{overall}}$  can be utilized to represent the overall efficiency of the VTOL mission, encompassing both dynamic and static conditions:

$$\eta_{\text{overall}} = \frac{P_{\text{aero}}}{P_{\text{mech}}} = \frac{\sum_{i=1}^{n} T_i V_i \zeta_i}{\sum_{i=1}^{n} \alpha_i \frac{T_i V_i}{n_i} \zeta_i + \sum_{i=1}^{n} \beta_i \tau_i \omega_i \zeta_i}.$$
(16)

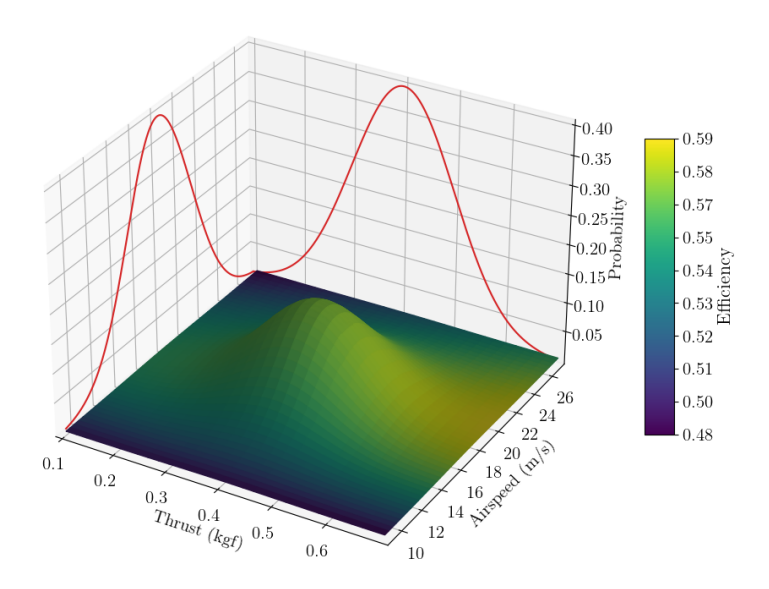


Figure 6 – Joint probability density function over the efficiency distribution for the 13x6.5 APC propeller at a single cluster.

## 3.2 Propeller Database Surrogate Modeling

In this research, we develop a propeller performance model using surrogate modeling techniques to reduce the computational cost of evaluating the efficiency of a large number of propellers. Surrogate modeling is an efficient approach for predicting engineering functions based on available data points within a defined parameter space. This methodology offers notable advantages in data analysis and

engineering design applications because it can significantly reduce the number of expensive computational simulations required, thus saving time and resources [16]. Specifically, in high-dimensional scenarios, surrogate models can effectively manage the exponential increase in computational resources needed for numerous evaluations of complex geometries and simulations [17]. However, it is important to note that high-dimensional surrogate models can face challenges such as reduced accuracy or difficulties in implementation due to the curse of dimensionality [17].

Among various surrogate modeling techniques, we select kriging as the surrogate model in this research, which can be called from the Python's SMT library<sup>2</sup>. Kriging is a form of Gaussian process regression (GPR) [18] and offers several advantages over other approaches. Firstly, kriging is a parametric technique that assumes a specific underlying distribution using the Gaussian process, simplifying the parameter estimation process. Secondly, kriging has the capability to generate spatially correct results [19], which enhances the accuracy of propeller performance predictions. These advantages make kriging a practical and efficient method for surrogate modeling of propeller data, particularly when working with experimental data. The methodology involves fitting a Gaussian process to the available data, which serves as a probabilistic model describing the data distribution. The Gaussian process is defined by a mean function and a covariance function, which determine the shape and behavior of the model.

An important step in kriging modeling is the tuning of hyperparameters, which is crucial to ensure the quality of the model. In this study, hyperparameter tuning is performed on a base propeller dataset consisting of approximately 500 data points for each propeller. The data is divided into 75% for training and the remaining portion for testing purposes, the visualization of this process is depicted in Fig. 7. This approach enables us to create a well-calibrated kriging model that delivers accurate predictions while maintaining computational efficiency.

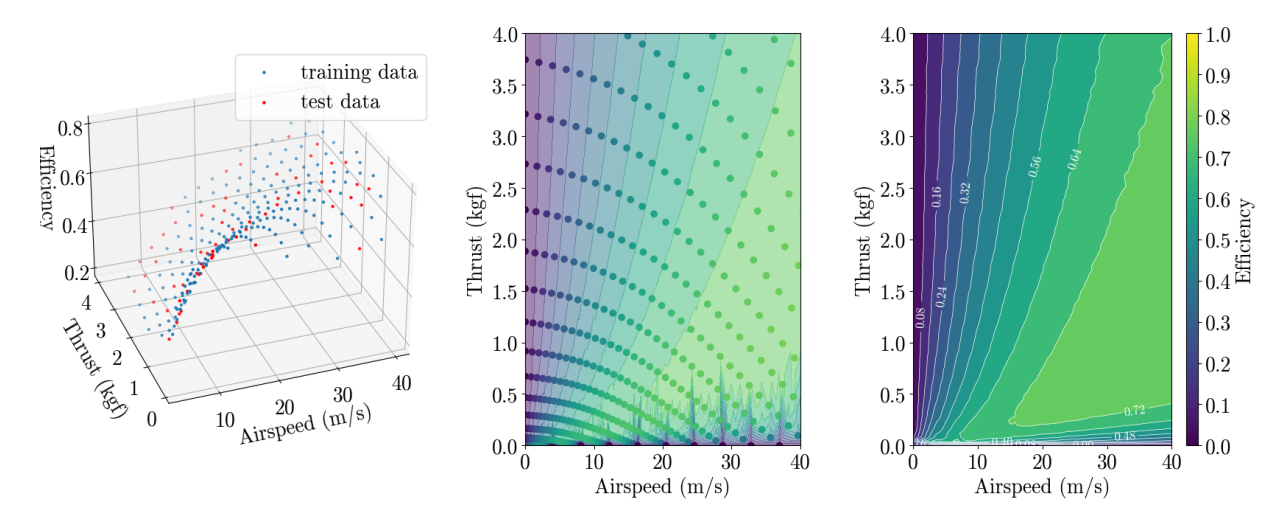


Figure 7 – Surrogate model process: visualization of training and test data (left), performance data of a propeller (middle), and the result of surrogate model showing the correlation between thrust, airspeed, and efficiency (right).

This research employs surrogate models using open-source propeller performance data, obtained from APC Propellers<sup>3</sup>, to predict the performance of multiple propellers for specified missions. The surrogate models enable efficient performance prediction by providing the relationship between a propeller's efficiency and its operational and design variables across numerous propellers. Furthermore, these models facilitate inverse calculations to obtain the required thrust from flight data, which is essential for optimization. By using these models, we can rapidly evaluate different design variables

 $<sup>^2</sup>$ https://smt.readthedocs.io/en/latest/\_src\_docs/surrogate\_models/krg.html (last accessed on 28 December 2023).

<sup>&</sup>lt;sup>3</sup>https://www.apcprop.com/technical-information/performance-data/ (last accessed on 09 November 2023).

and mission profiles, significantly reducing the computational time needed for optimization. This process allows us to optimize the overall efficiency of the propellers across a wide range of designs and mission profiles.

# 3.3 Optimal Propeller Selection

The optimal propeller selection in this study is a determination of the most efficient propeller for a VTOL sUAV fixed-wing aircraft in multiple-diverse missions. The selection process involves the evaluation of the performance of various propellers using flight data analysis, surrogate modeling techniques, and mission analysis.

The obtained propeller performance data of each propeller are used to form a surrogate model. The surrogate model is then used to determine the optimal solution for the propeller selection. The optimal solution is obtained by evaluating the overall efficiency of each propeller, and the propeller with the highest predicted overall efficiency is selected.

In the process of determining the optimal solution, we aim to maximize the overall efficiency of a propeller,  $\eta_{\text{overall}}$ , with respect to the propeller diameter D and pitch Pi.  $\eta_{\text{overall}}$  is influenced by the thrust  $T_i$ , airspeed  $V_i$ , mechanical power  $P_{\text{mech}i}$ , and time duration  $\zeta_i$  at each flight segment, i, which enables the consideration of the different mission profiles. We examine two types of optimization problems: a discrete optimization problem, where D and Pi must be chosen from a predefined set of propellers (referred to as the "Propeller Set"), and a continuous optimization problem with no restrictions on the choice of  $D \in \mathbb{R}$  and  $Pi \in \mathbb{R}$ .

# Discrete Optimization Problem

In this case, the goal is to select the best propeller from a finite set based on its overall efficiency across all mission segments, providing available solution from propeller set. The formulation of the discrete optimization problem to obtain the optimal selection point is as follows:

$$\begin{array}{ll} \text{maximize} & \eta_{\text{overall},j} \\ & j \\ \text{subject to} & D_j, Pi_j \in \text{Propeller Set}, \end{array} \tag{17}$$

where:

- *j* is the index of the propellers in the finite selection;
- $D_i$  is the diameter of the propeller for the j-th propeller;
- *Pi*<sub>j</sub> is the pitch of the propeller for the *j*-th propeller;
- $\eta_{\text{overall},j}$  is the overall efficiency for the *j*-th propeller.

## Continuous Optimization Problem

In this case, the diameter and pitch of the propeller can take any arbitrary value within specified bounds, aiming to maximize the overall efficiency by performing global optimization. The formulation of the continuous optimization problem to obtain the global optimal point is as follows:

$$\begin{array}{ll} \underset{D,Pi}{\text{maximize}} & \eta_{\text{overall}}(D,Pi) \\ \text{subject to} & D_{\min} \leq D \leq D_{\max} \\ & Pi_{\min} \leq Pi \leq Pi_{\max}, \end{array}$$

where:

- *D* is the diameter of the propeller (continuous variable);
- *Pi* is the pitch of the propeller (continuous variable);
- $\eta_{\text{overall}}(D,P)$  is the overall efficiency across all mission segments.

# 4 Test Case Study and Results

In this section, we present an in-depth analysis of a test case and the results from our proposed methodology. The objective is to highlight the potential improvement in overall efficiency by applying mission-based optimal propeller selection methodology.

# 4.1 Setup Case

To test and observe the implementation of the proposed methodology, the test aircraft was flown on a typical aerial mapping mission with a simple grid configuration as depicted in Fig. 4b, covering a certain area. The overall mission profile follows the regular aerial mapping flight pattern for VTOL sUAV that consists of vertical take-off, climb, cruise, descent, and followed by vertical landing.

The VTOL sUAV demonstrates unique characteristics during take-off and landing. These phases are executed through a combination of vertical hovering and forward flight transitioning, distinguishing it from conventional aircraft. The cruising phase of the VTOL sUAV also displays a distinct feature compared to conventional aircraft. The VTOL sUAV is required to perform multiple 180° turns throughout the flight. This requirement is due to the specific needs of the aerial mapping mission, which necessitates extensive coverage of a certain area. This characteristic makes the cruising phase of the VTOL sUAV different from that of conventional aircraft. The entire flight profile is shown in Fig. 8.

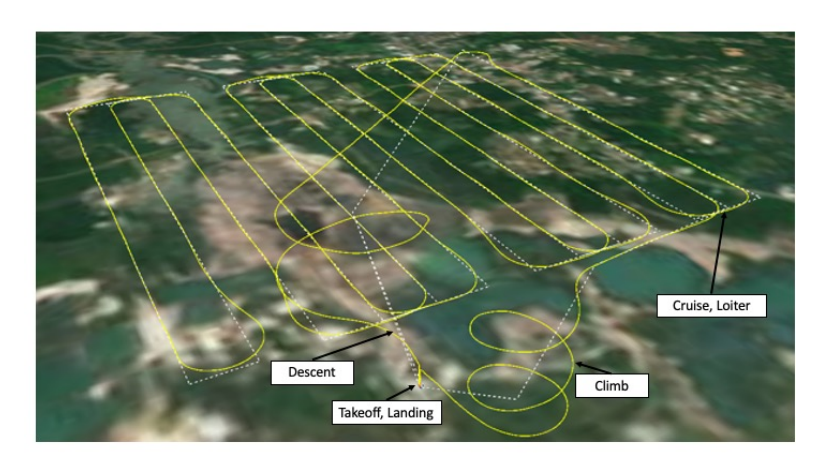


Figure 8 – Flight trajectory for the entire mission of a test flight.

The configuration of the aircraft being used during the test flight is the tilt-rotor type the Raybe from BETA company, which is shown in Fig. 1b. The detailed specifications of the aircraft being used during the test flight are described in Table 1.

When retrieving flight data, the raw flight data record can be seen in Fig. 9. The data were measured by the flight controller at 10Hz, resulting in nearly 10,000 data points. Although the flight data could give very dense detailed information, interpreting the flight data is a very complex task and often does not directly give insight into the flight condition.

Table 1 – The specifications of the BETA Raybe used in test flights.

Parameter	Value
Aircraft type	Tilt-rotor
Maximum take-off weight	5,200 g
Wingspan	1,830 mm
Length	1,270 mm
Cruising speed	17.5 m/s
Stall speed	13 m/s
Transition height	30–50 m

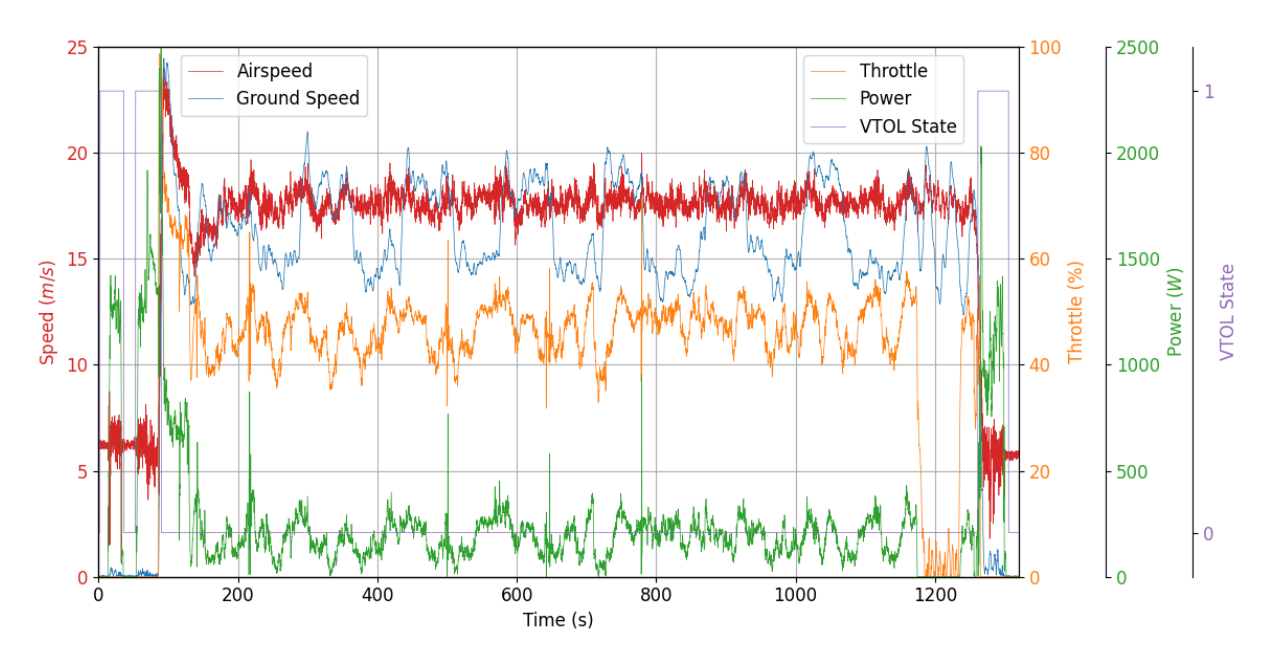


Figure 9 – Time series airspeed (red), ground speed (blue), throttle (orange), power(green), and VTOL state (purple) data of the test case.

# 4.2 Flight Data Analysis

The initial step of the flight data analysis is to obtain the scattered flight condition data, which are the dataset of correlation between the airspeed and the thrust as shown in Fig. 5. The initial scattered flight condition is obtained by combining the raw flight data with the surrogate model of the installed propeller or the base propeller to obtain the required thrust.

Based on the autopilot control information, the flight is further segmented into the VTOL phase and the cruising phase. Then, an initial clustering is performed using the HDBSCAN algorithm to obtain the estimated number of clusters for each flight.

From the initial result of the HDBSCAN process, as seen in Fig. 10, the clusters are distinctive and represent conditions during the three phases. During the take-off phase, the purple cluster represents the vertical take-off condition, while the more sparse yellow cluster represents the transition condition. A similar pattern is observed during the landing phase, differing only in the number of clusters. Specifically, there are two additional clusters for landing, which correspond to the re-transitioning from fixed-wing to VTOL configuration. This transition, involving both soft and hard braking, is unique to the landing process. In addition, the autopilot needs to confirm the final landing condition before shutting all engines off, resulting in a small cluster depicted at the bottom left corner of the landing phase.

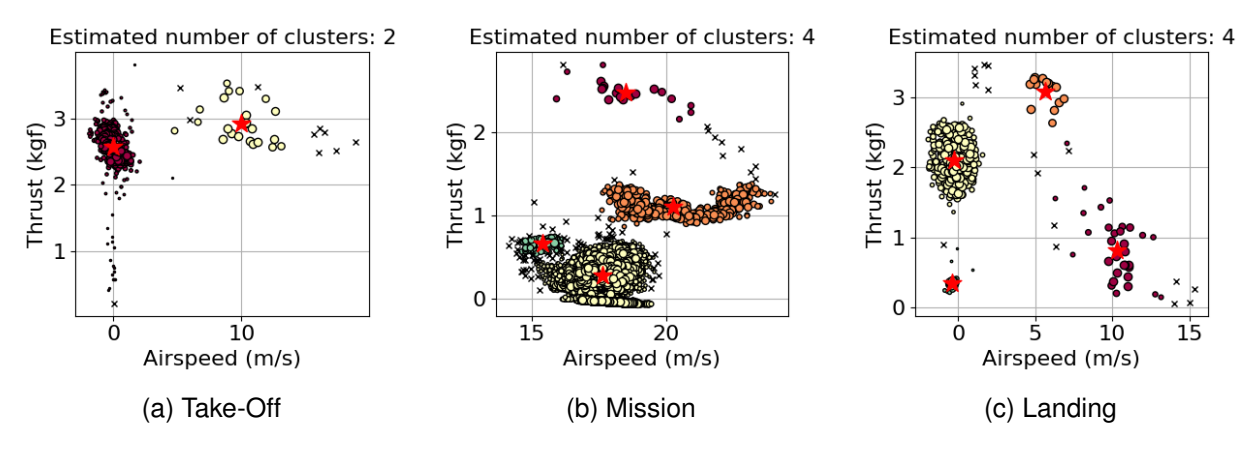


Figure 10 – Estimation of cluster numbers using HDBSCAN for take-off, mission, and landing phases.

Additionally, the initial clustering of the mission phases provides insight into the flight conditions during the mission. For the mission phase, the biggest yellow cluster represents the condition during the cruise, with a mean average airspeed value equal to the aircraft's cruising speed at  $17.5\,\mathrm{m/s}$ . Another cluster, with a high thrust requirement and high speed, likely corresponds to the climb condition. The other cluster, with a higher thrust requirement and low speed, might correspond to turning. Although these claims need to be validated by more advanced techniques in the future, the initial clustering by HDBSCAN is shown to be promising in identifying patterns and characteristics within extensive flight data. The clustering also enables the segmentation of the full mission into distinctive parts for further computation.

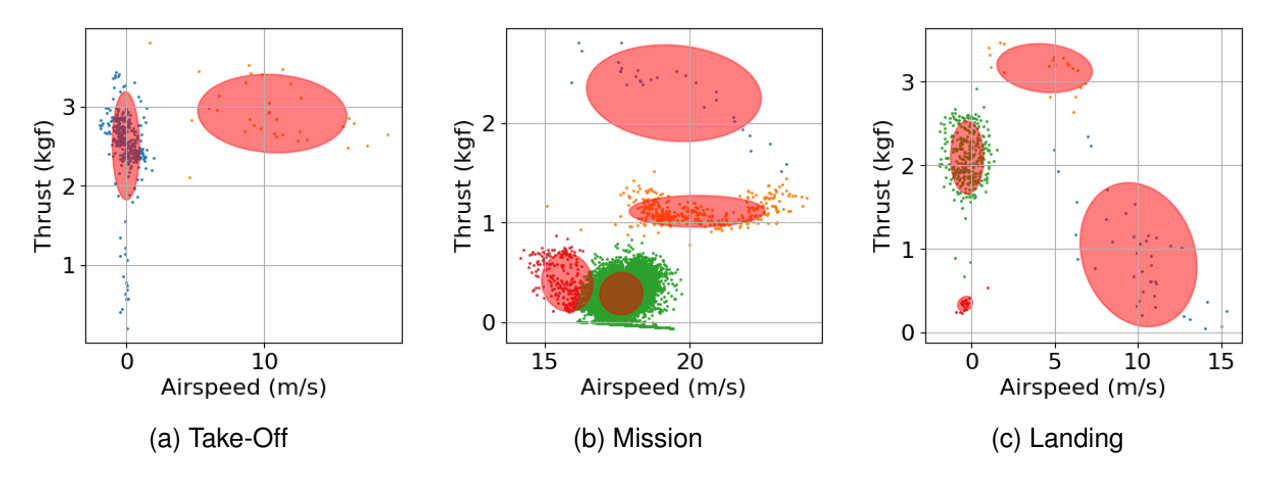


Figure 11 – Re-clustering using the GMM.

Based on the result of the cluster number estimation using HDBSCAN, the flight data are re-clustered by the GMM algorithm to obtain means and standard deviations from each cluster, which is assumed to follow a Gaussian distribution. The information is then used as the flight loads to analyze the clustered flight load distribution as shown in Fig. 5.

From the whole clustering process, the flight load distribution is properly examined as Fig. 13. Although the sUAV configuration is designed to perform as a VTOL and fixed-wing aircraft, the VTOL phase only accounted for 2.9% and 3.2% of the total flight time during the take-off and landing phases, respectively, while the mission or cruise phase contributed 93.9%, as seen in Fig. 12. The combination for these distributions is highly dependent on the mission requirements and flight conditions. In further examination of each cluster, we observed that each flight segment is dominated by one cluster, hovering for both take-off and landing, and cruise for the mission segment. Hypothetically, this could lead to further data reduction; however, as the current computational cost is reasonably low, further reduction is unnecessary in this current study.

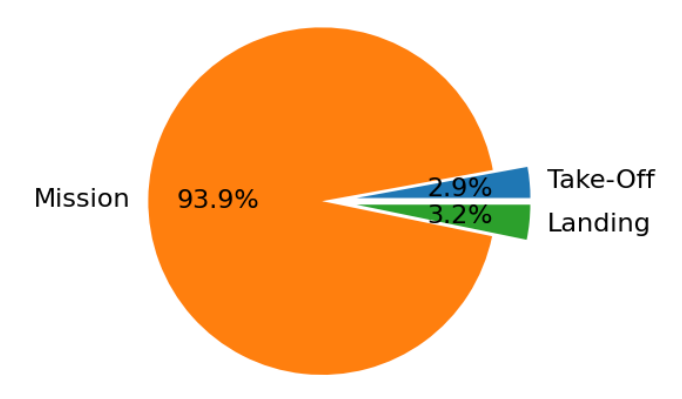


Figure 12 – The percentage of each flight segement for test case.

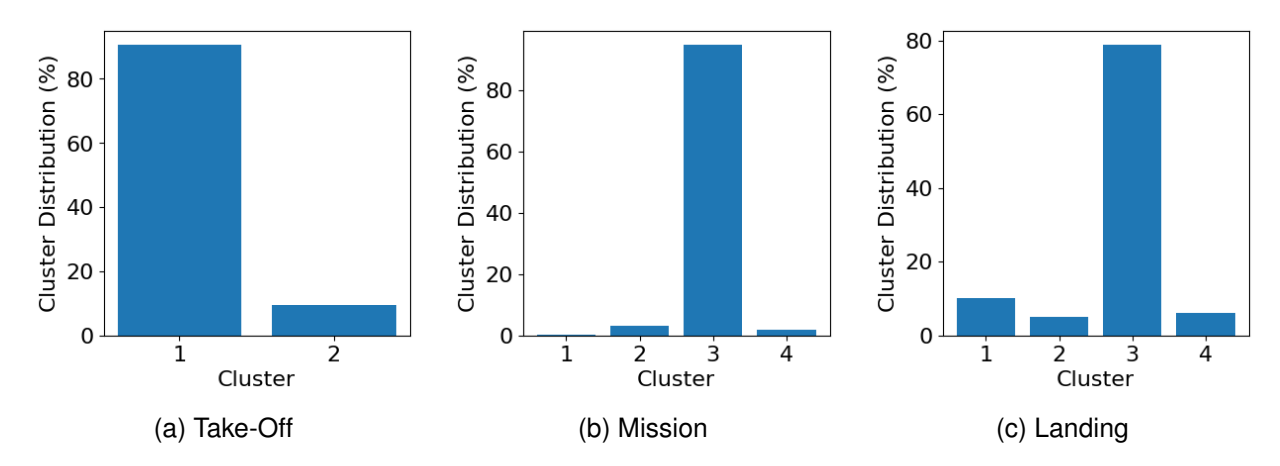


Figure 13 – Proportion of data points in each cluster during take-off, mission, and landing phases.

# 4.3 Optimal Propeller Selection and Improvement Evaluation

Following the methodology described in Fig. 5, and after rigorously evaluating the efficiency of all propellers in the dataset using Eq. (16), an efficiency contour map varying with the propeller pitch and diameter is built using a kriging model. Figure 14 shows the efficiency contour map of the two evaluated conditions: excluding the take-off and landing phases, as in normal fixed-wing aircraft (left), and full mission analysis including VTOL aspects (right).

The optimal propeller selection is performed by comparing three conditions: the base propeller, the optimal selection point, and the global optimal point. The optimal selection point indicates the best efficiency obtainable from the available selections (the result of solving Eq. (17)), while the global optimal point demonstrates the maximum efficiency attainable by fabricating a custom propeller (the result of solving Eq. (18)).

By considering only the cruise phase (the results shown on the left side of Fig. 14), the optimal selection point was found to be at 13x14, and the global optimal point was at 14x15.7. Compared to the existing base propeller, 13x8, the expected improvements in this flight phase are 13.2% for the optimal selection and 13.3% for the global optimal point, indicating a further potential improvement of 0.7% over the selection of the existing propeller.

Furthermore, by considering the take-off and landing phases in the full mission analysis (the results shown on the right side of Fig. 14), the probable *optimal selection* shifted to a higher diameter propeller, resulting in 19x16 with an 11.8% overall performance increase compared to *the base propeller*. Compared with the previous optimal selection obtained only with the cruise phase analysis, 13x14 improved the overall efficiency by 5.4%. Additionally, *the global optimal point*, located at 18.5x16.2, showed a 12% improvement over *the base propeller*, or 1.7% over *the optimal selection point*.

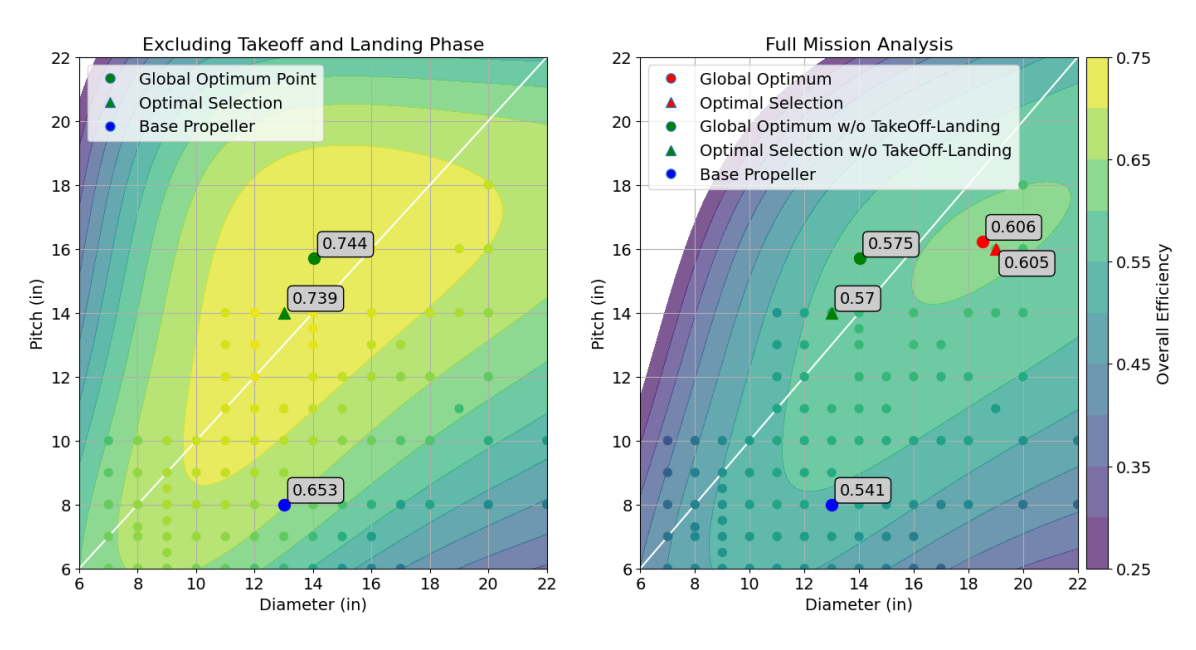


Figure 14 – The standard APC propellers' overall efficiency map depending on the propeller diameter and pitch, for mission phases excluding take-off and landing (left) and for a full mission (right).

The change in the required diameter and pitch of the propeller when considering the full mission can be analyzed by observing the contour of efficiency using the TPR (see Eq. (2)) in the vertical take-off and landing condition, as depicted in Fig. 15. The higher TPR indicates the propeller generates more thrust for the same power, improving efficiency. The TPR increases as the diameter of the propeller increases and decreases as the pitch of the propeller increases. Therefore, a larger diameter and a lower pitch are the preferred propeller configurations at this stage, although there may be limits to these values.

Comparing the three propellers: the base propeller has a TPR of 7.3 g/W, while the optimal selection point without take-off and landing phases has a 19.7% lower value and the optimal selection point from full mission analysis has a 23.7% higher value. The decrease in the optimal selection point without take-off and landing phases is due to omitting the take-off and landing requirements. Consequently, the optimizer strives for better efficiency during cruise conditions by increasing the pitch of the propeller. On the other hand, the full mission analysis consider both situations, resulting in optimizing both variables to achieve the highest overall efficiency. However, compared to the optimal result of excluding the take-off and landing phases, the increase is only noticeable in the higher diameter required. This might imply that these conditions, which are unique to a VTOL aircraft, make the optimizer prefer a larger diameter for better efficiency, while a higher pitch is more desirable for cruising.

Moreover, the results from the full mission analysis show a significant improvement over the cruise phase analysis, yielding a 6.4% better improvement in the test condition. This highlights the importance of performing a full mission analysis to properly address the selection in the VTOL platform.

# 5 Conclusion

In conclusion, the studies discussed in this paper propose new approaches for selecting optimal propellers for convertible tilt-rotor sUAVs that consider the entire flight operating spectrum of the vehicle. The proposed methodologies provided a quantitative basis for rigorous propeller selection, aiming to improve the overall performance throughout the vehicle's operations. By overcoming the challenges of mission-based analysis in sUAVs, such as large amounts of data and measurement

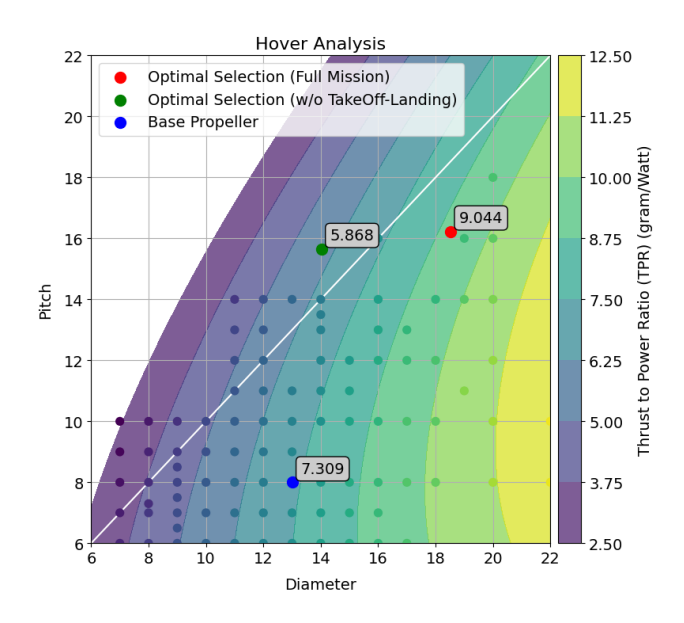


Figure 15 – Thrust to power ratio of standard APC propellers.

uncertainties, our works provided practical solutions for propeller selection. These studies contribute to the field of sUAV development and have the potential to improve the efficiency and effectiveness of sUAV operations in various applications.

Although the percentage of performance improvement might vary depending on the specific mission specification, the proposed work could demonstrate an optimal selection method that could yield better performance for any flight and mission requirements based on the actual flight data. This paper also provided both detailed and qualitative performance evaluations throughout the proposed optimal selection process, enabling users to swiftly reach a suitable propeller selection to improve mission efficiency.

Future work would focus on incorporating the flight operation aspect into the optimization process to achieve better overall efficiency from both the aircraft aerodynamics and the propeller. Additionally, the design variables in the optimization process would be extended to account for different types of propellers. Improving the optimization methodology to enhance computational efficiency is also planned, to support real-time applications using mobile platforms or even handheld devices. We acknowledge that the present work might still have limitations in that there may be discrepancies between the real and predicted results due to unaccounted-for propeller-fuselage interactions and calibration factors in sensor readings. With more case studies explored (with different configurations, mission specifications, and operating conditions), we would be able to further validate and improve the functionalities of our approaches.

### **Acknowledgement**

We would like to acknowledge the support from the Hong Kong PhD University Grant Council of the Hong Kong Special Administration Region for providing financial support to the first author through the Hong Kong PhD Fellowship Scheme (HKPFS).

# **Copyright Statement**

The authors confirm that they, and/or their company or organization, hold copyright on all of the original material included in this paper. The authors also confirm that they have obtained permission, from the copyright holder of any third party material included in this paper, to publish it as part of their paper. The authors confirm that

they give permission, or have obtained permission from the copyright holder of this paper, for the publication and distribution of this paper as part of the ICAS proceedings or as individual off-prints from the proceedings.

## References

- [1] Sarvesh Sonkar, Prashant Kumar, Deepu Philip, and AK Ghosh. Low-cost smart surveillance and reconnaissance using vtol fixed wing uav. In 2020 IEEE Aerospace Conference, pages 1–7. IEEE, 2020.
- [2] D Rakesh, N Akshay Kumar, M Sivaguru, KVR Keerthivaasan, B Rohini Janaki, and R Raffik. Role of uavs in innovating agriculture with future applications: A review. In *2021 International Conference on Advancements in Electrical, Electronics, Communication, Computing and Automation (ICAECA)*, pages 1–6. IEEE, 2021.
- [3] Mingjie Zhou, Zhiyan Zhou, Luohao Liu, Jun Huang, and Zichen Lyu. Review of vertical take-off and landing fixed-wing uav and its application prospect in precision agriculture. *International Journal of Precision Agricultural Aviation*, 3(4), 2020.
- [4] Nourhan Elmeseiry, Nancy Alshaer, and Tawfik Ismail. A detailed survey and future directions of unmanned aerial vehicles (uavs) with potential applications. *Aerospace*, 8(12):363, 2021.
- [5] Henry V. Borst. The Design and Selection of Optimum Propellers for General Aviation Aircraft. In *Business Aircraft Meeting and Exposition*. SAE International, February 1979. ISSN: 0148-7191.
- [6] Yamika Patel, Anant Gaurav, Krovvidi Srinivas, and Yamal Singh. A review on design and analysis of the propeller used in UAV. *Int. J. Adv. Prod. Ind. Eng*, 605:20–23, 2017.
- [7] Wayne Johnson and Christopher Silva. Observations from exploration of vtol urban air mobility designs. In *Asian/Australian Rotorcraft Forum (ARF 2018)*, 2018. Issue: ARC-E-DAA-TN60637.
- [8] Zairil Zaludin and Ahmad Salahuddin Mohd Harituddin. Challenges and Trends of Changing from Hover to Forward Flight for a Converted Hybrid Fixed Wing VTOL UAS from Automatic Flight Control System Perspective. In 2019 IEEE 9th International Conference on System Engineering and Technology (ICSET), pages 247–252, October 2019. ISSN: 2470-640X.
- [9] Ugur Ozdemir, Yucel Orkut Aktas, Aslihan Vuruskan, Yasin Dereli, Ahmed Farabi Tarhan, Karaca Demirbag, Ahmet Erdem, Ganime Duygu Kalaycioglu, Ibrahim Ozkol, and Gokhan Inalhan. Design of a Commercial Hybrid VTOL UAV System. *Journal of Intelligent & Robotic Systems*, 74(1):371–393, April 2014.
- [10] Pavlos E. Kaparos, Chris D. Bliamis, and Kyros Yakinthos. Conceptual design of a UAV with VTOL characteristics. In *AIAA Aviation 2019 Forum*, AIAA AVIATION Forum. American Institute of Aeronautics and Astronautics, June 2019.
- [11] Guillaume J. J. Ducard and Mike Allenspach. Review of designs and flight control techniques of hybrid and convertible VTOL UAVs. *Aerospace Science and Technology*, 118:107035, 2021.
- [12] Akshat Misra, Sudhakaran Jayachandran, Shivam Kenche, Anirudh Katoch, Arjun Suresh, Edison Gundabattini, Senthil Kumaran Selvaraj, and Addisalem Adefris Legesse. A Review on Vertical Take-Off and Landing (VTOL) Tilt-Rotor and Tilt Wing Unmanned Aerial Vehicles (UAVs). *Journal of Engineering*, 2022:1803638, September 2022. Publisher: Hindawi.
- [13] Jonas Hippe, Felix Finger, Falk Götten, and Carsten Braun. Propulsion System Qualification of a 25 kg VTOL-UAV: Hover Performance of Single and Coaxial Rotors and Wind-Tunnel Experiments on Cruise Propellers. In *Deutscher Luft- und Raumfahrtkongress DLRK 2020*, 2020.
- [14] Pasquale M. Sforza. Chapter 10 Propellers. In Pasquale M. Sforza, editor, *Theory of Aerospace Propulsion (Second Edition)*, Aerospace Engineering, pages 487–524. Butterworth-Heinemann, second edition edition, 2017.
- [15] Datong Liu, Ning Xiao, Yujie Zhang, and Xiyuan Peng. Unsupervised Flight Phase Recognition with Flight Data Clustering based on GMM. In *2020 IEEE International Instrumentation and Measurement Technology Conference (I2MTC)*, pages 1–6, 2020.
- [16] Pramudita Satria Palar, Rhea Patricia Liem, Lavi Rizki Zuhal, and Koji Shimoyama. On the use of surrogate models in engineering design optimization and exploration: The key issues. In *Proceedings of the genetic and evolutionary computation conference companion*, pages 1592–1602, 2019.
- [17] Chun Hou and Kamran Behdinan. Dimensionality Reduction in Surrogate Modeling: A Review of Combined Methods. *Data Science and Engineering*, 7, August 2022.
- [18] M. A. OLIVER and R. WEBSTER. Kriging: a method of interpolation for geographical information systems. *International journal of geographical information systems*, 4(3):313–332, 1990.
- [19] Gowtham Atluri, Anuj Karpatne, and Vipin Kumar. Spatio-temporal data mining: A survey of problems and methods. *ACM Computing Surveys (CSUR)*, 51(4):1–41, 2018.